The effect of surface pre-conditioning treatments on the local composition of Zr-based conversion coatings formed on aluminium alloys

Cerezo Palacios, JM; Vandendael, I.; Posner, R; de Wit, JHW; Mol, JMC; Terryn, HA

DOI
10.1016/j.apsusc.2016.01.106

Publication date
2016

Document Version
Final published version

Published in
Applied Surface Science

Applied Surface Science 366 (2016) 339–347

Contents lists available at ScienceDirect

Applied Surface Science

journal homepage: www.elsevier.com/locate/apsusc

The effect of surface pre-conditioning treatments on the local composition of Zr-based conversion coatings formed on aluminium alloys

J. Cerezo[a,b], I. Vandendael[c], R. Posner[d], J.H.W. de Wit[b], J.M.C. Mol[b,*], H. Terryn[a,b,c]

[a] Materials innovations institute (M2i), Mekelweg 2, Delft, 2628 CD, The Netherlands
[b] Delft University of Technology, Department of Materials Science and Engineering, Mekelweg 2, Delft, 2628 CD, The Netherlands
[c] Vrije Universiteit Brussel, Research Group of Electrochemical and Surface Engineering, Pleinlaan 2 Brussels, B-1050, Belgium
[d] Henkel AG & Co. KGaA, Henkelstr. 67, 40589 Dusseldorf, Germany

ARTICLE INFO

Article history:
Received 6 August 2015
Received in revised form 9 November 2015
Accepted 13 January 2016
Available online 14 January 2016

Keywords:
Zr-based conversion coatings
Aluminium alloys
FE-AES
Surface treatments
Copper enrichment

ABSTRACT

This study investigates the effect of different alkaline, acidic and thermal pre-conditioning treatments applied to different Al alloy surfaces. The obtained results are compared to the characteristics of Zr-based conversion coatings that were subsequently generated on top of these substrates. Focus is laid on typical elemental distributions on the sample surfaces, in particular on the amount of precipitated functional additives such as Cu species that are present in the substrate matrix as well as in the conversion bath solutions. To this aim, Field Emission Auger Electron spectra, depth profiles and surface maps with superior local resolution were acquired and compared to scanning electron microscopy images of the sample. The results show how de-alloying processes, which occur at and around intermetallic particles in the Al matrix during typical industrial alkaline or acidic cleaning procedures, provide a significant source of crystallization cores for any following coating processes. This is in particular due for Cu-species, as the resulting local Cu structures on the surface strongly affect the film formation and compositions of state-of-the-art Zr-based films. The findings are highly relevant for industrial treatments of aluminium surfaces, especially for those that undergo corrosion protection and painting process steps prior to usage.

1. Introduction

Conversion treatments are commonly employed in the manufacturing process of metallic components to reduce the corrosion susceptibility and to increase the adhesion performance of organic coatings to these substrates [1–9]. The process depends on the transformation of the native oxide layer on the substrate material into a functional coating film, typically due to the precipitation of phosphate crystals or of amorphous metal oxides from solution.

Currently, Zr- and Ti-based thin film technology more and more replaces conventional phosphating due to several advantages regarding costs, easy process control, reduced energy consumption and the avoidance of extensive wastewater treatment protocols. State-of-the-art conversion coating often relies on the properties of fluoric acids of zirconium and titanium, mediated by diverse functional additives to ensure desired thin film structures on various metals such as steel, galvanized steel and aluminium. The resulting coatings typically achieve a thickness of not more than 20–100 nm and are mainly composed of TiO_2/ZrO_2 [10].

Upon immersion of the metal substrate in the conversion bath, the Zr deposition process starts with the chemical dissolution of the oxide layer by free fluoride. For aluminium alloys, the effectivity of this step is highly determined by the surface chemistry of the oxide layer. In particular, it is strongly dependent on the conditions of any surface pre-conditioning such as acidic, neutral or alkaline cleaning steps which are typically part of the industrial manufacturing processes. For example, Cerezo et al. [11] recently suggested that high hydroxyl fractions on AA6014 favors the chemical dissolution of the oxide layer and significantly impacts the composition of any subsequently precipitated Zr-based conversion coating. Such precipitation is triggered by the local alkalinization of the metal/solution interface and the increase in pH is promoted by oxygen reduction and hydrogen evolution reactions [12,13]. For aluminium alloys, several authors reported that these reactions are

* Corresponding author. Tel.: +31 15 2786778; fax: +31 2786730.
E-mail address: J.M.C.Mol@tudelft.nl (J.M.C. Mol).

http://dx.doi.org/10.1016/j.apsusc.2016.01.106
0169-4332/

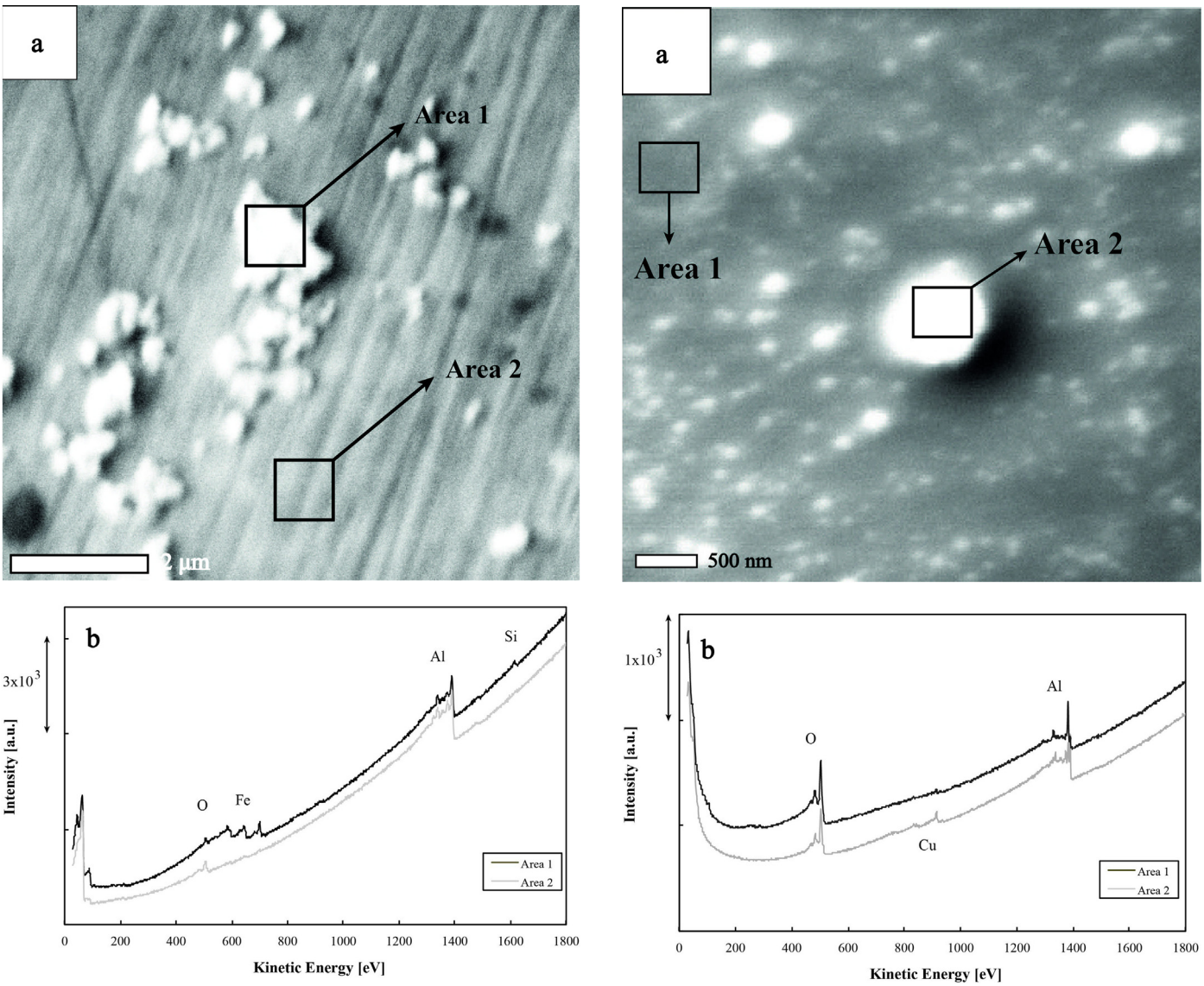

Fig. 1. (a) SEM micrograph of the AA6014 reference sample. (b) Localized FE-AES spectra at two different zones of the sample.

Fig. 2. (a) SEM micrograph of the AA6014 alkaline treated specimen. (b) FE-AES spectra at two different areas of the specimen.

predominant on the cathodic intermetallic particles, and therefore the deposition starts at these sites [14–16]. Once a covering film is achieved, an increase in the thickness occurs during longer immersion times [13]. Adhikari et al. [17] used the Quartz Crystal Microbalance to prove that the growth rate of the Zr-based coating on different metals is accelerated by the addition of Copper ions to the conversion bath solution. X-ray Photoelectron Spectroscopy studies carried out by Lostak et al. [18] confirmed an increase of the film thickness under these conditions. The acceleration mechanism is based on the deposition of Cu by displacement reactions, which provide additional cathodic sites for local alkalinization at the surface. Cerezo et al. [19] reported that the amount of Cu within the conversion film strongly depends on the type of substrate on which the coating is formed. In a recent work, Sarfraz et al. [20] investigated the role of the intermetallics and of copper ions present in a fluorozirconic acid solution for the deposition of Zr-oxide based coatings on alkaline pre-conditioned AA6014 surfaces. A preferential deposition of Cu on top of the intermetallics present at the surface was proven and emphasized the locally inhomogenous structure of conversion layers on aluminium.

The present study extends this approach. Determined by the type of Al alloy, Cu is already present in the aluminium matrix and/or part of the elemental composition of the intermetallic particles. Prior to an immersion in the conversion solution, alkaline and/or acidic surface conditioning treatments are commonly applied to remove organic contaminants. Thereby, aged oxide films are removed by freshly grown oxide layers which also exhibit specific reactivity towards subsequent conversion coating. During this process, the local elemental composition on the substrate surface gets modified in the micron and sub-micron range. Depending on the type of pre-conditioning, a release of functional species will occur, which may result in an additional source for Cu crystallization cores across the substrate surface. In other words, it has to be expected that the cleaning stage prior to the conversion treatment will pre-determine the distribution and a possible local enrichment of active Cu sites. Those sites, in turn, will impact the subsequently generated Zr-oxide layer structure as well as its thickness.

Unfortunately, such effects were not investigated in detail so far. As a consequence, potential optimizations of the related industrial manufacturing processes were not exploitable up to now. In this context, the present publication will provide a significant

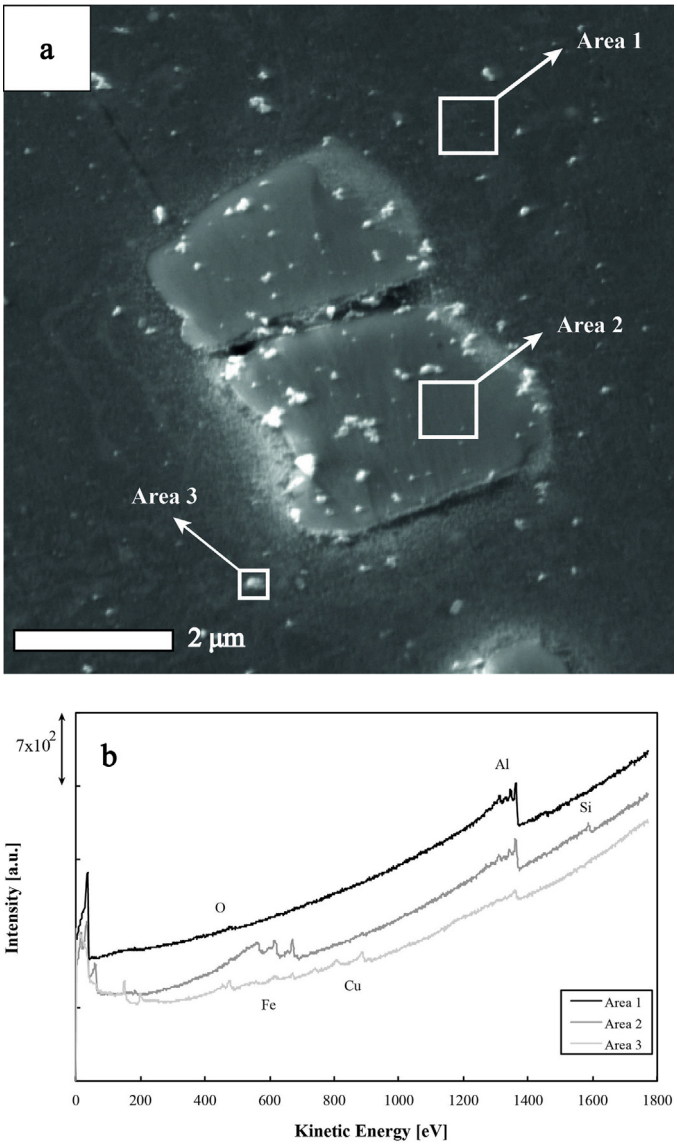

Fig. 3. (a) SEM micrograph of the AA6014 acid treated samples. (b) FE-AES spectra at three different zones of the specimen.

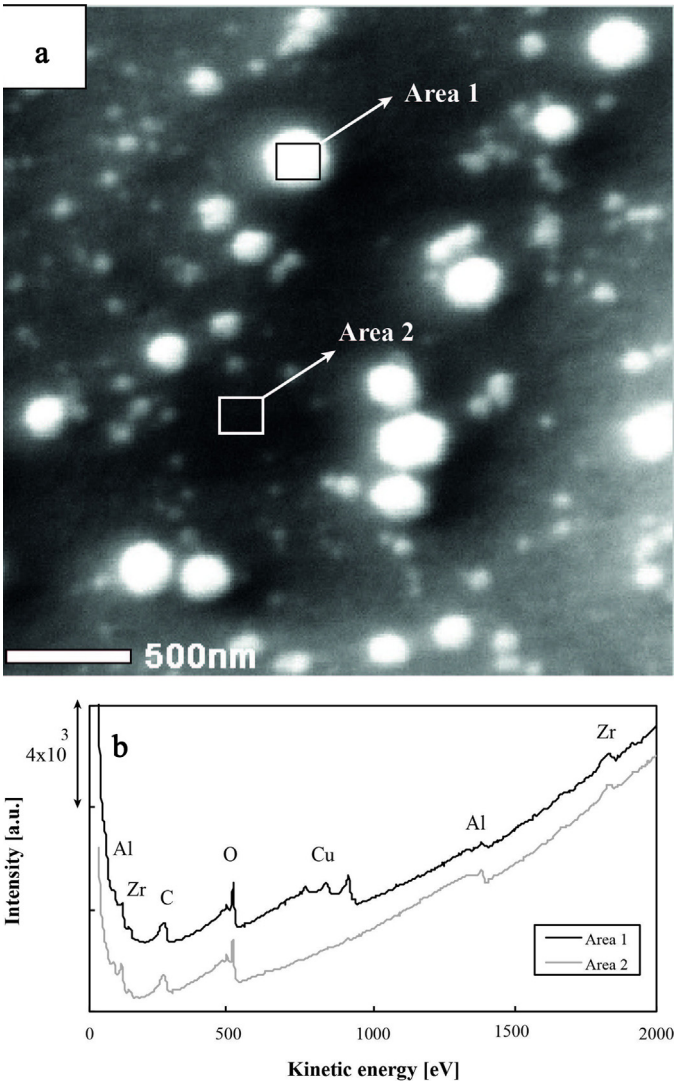

Fig. 4. (a) SEM micrograph of the Zr-based conversion coating deposited on the AA6014 alkaline treated specimen. (b) FE-AES spectra at two different areas of the sample.

contribution to a better understanding. Therefore, different model conditioning treatments were applied on Al alloys in order to form well-defined oxide films with similar oxide layer thickness and different hydroxyl fractions prior to immersion in the Cu-containing Zr-based conversion solution. Please note that the oxide film chemistry and thickness of the different aluminium surfaces evaluated in this study were already reported by Cerezo et al. [11]. Field Emission Auger Electron Spectroscopy (FE-AES) was used to acquire high-resolution surface maps, localized spectra and depth profiles as well as to characterize the elemental distribution of the specimens before and after the formation of the Zr-based conversion coatings.

2. Experimental

Sheets of AA6014 and AA1050 aluminium alloys provided by Henkel AG & Co. KGaA and Goodfellow respectively were used in this study. AA6014 contains Mg ≤0.8 wt.%, Fe ≤0.35 wt.%, Si ≤0.6 wt.%, Cu ≤0.2 wt.%, Mn ≤0.2 wt.% as alloying elements. On the other hand, AA1050 is composed of Al ≥ 99.5 wt%, Fe ≤ 0.3 wt.%, Si ≤ 0.2 wt.%. All the specimens were mechanically ground with SiC paper and polished in subsequent steps to different grade diamond paste (9, 6, 3, 1, and 0.25 μm). Then, the samples were ultrasonically degreased in ethanol for five minutes and dried in compressed air. Subsequently, the from now on called reference sample was exposed to an acid, alkaline or thermal treatment. The acid treatment was composed of the immersion of the samples for 30 s in a 30 vol.% nitric acid solution. This was followed by 3 min rinsing in deionized water and drying with compressed air. For the alkaline treatment, the samples were dipped in a 3 vol.% potassium hydroxide solution at 57 °C with a stirring rate of 150 rpm for 3 min. The pH of this solution was adjusted to 10.8 at 57 °C with phosphoric acid at 10 vol.%. For the thermal treatment the specimens were heated in air at a temperature of 275 °C for 24 h.

To form Zr-based conversion coatings, samples were dipped into a modified hexafluorozirconic acid solution (Zr < 200 mg/l) that included smaller amounts (<50 mg/l) of non-hazardous components of Cu [17,19] provided by Henkel AG & Co. KGaA. Treatment occurred in a 1 L-beaker during 90 s in stirred solution (employing a stirring bar at 400 rpm) with a pH of 4 (adjusted by 15 vol% ammonium bicarbonate). Afterwards, the samples were rinsed with deionized water and dried with compressed air.

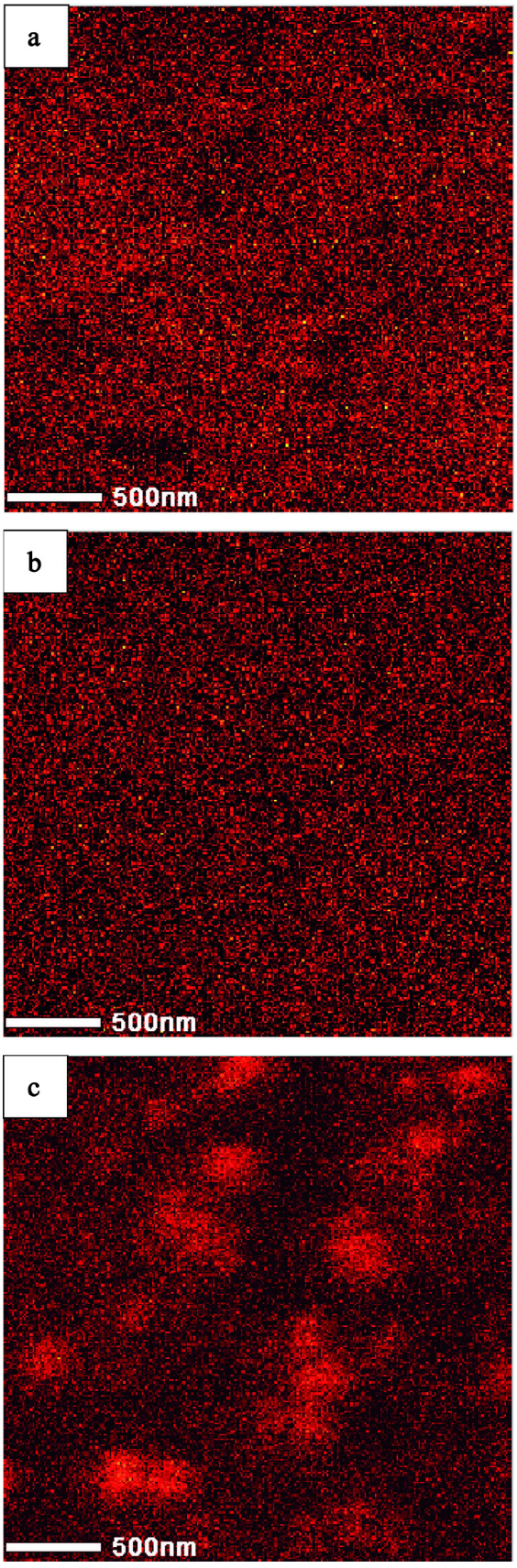

Fig. 5. FE-AES (a) Zr, (b) Al, (c) Cu map of the Zr-based conversion coating formed on the AA6014 alkaline treated sample.

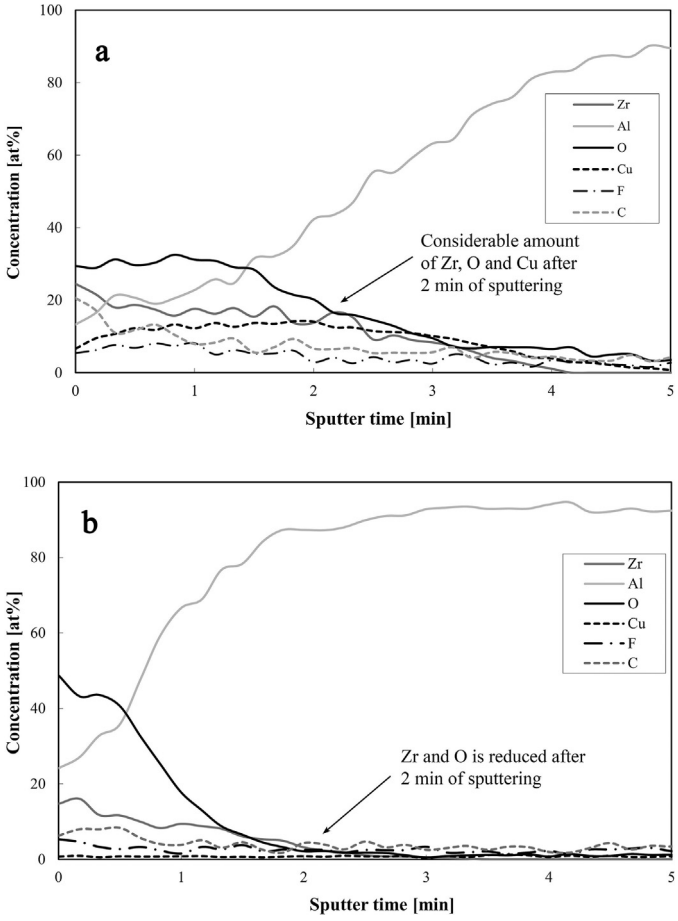

Fig. 6. Localized FE-AES depth profiles of the Zr-based conversion film deposited on the AA6014 alkaline treated specimen on (a) a Cu-rich zone and (b) a zone without Cu.

The surface analysis before and after the formation of the Zr-based conversion coating was conducted with a JEOL 9500F JAMP Scanning Auger Microprobe. For that purpose, an electron beam of 10 kV, 1 nA and 8 nm in diameter was applied at an angle of incidence of 30° with respect to the sample surface normal. When carbon was detected at the surface, the sample was sputtered with 1 KeV Ar^+ ions to remove the contamination. Scanning Electron Microscopy (SEM) images of the studied area were acquired using a secondary and a backscattered electron detector attached to the FE-AES system. For all the samples, localized FE-AES spectra were acquired in different zones. Surface maps were recorded

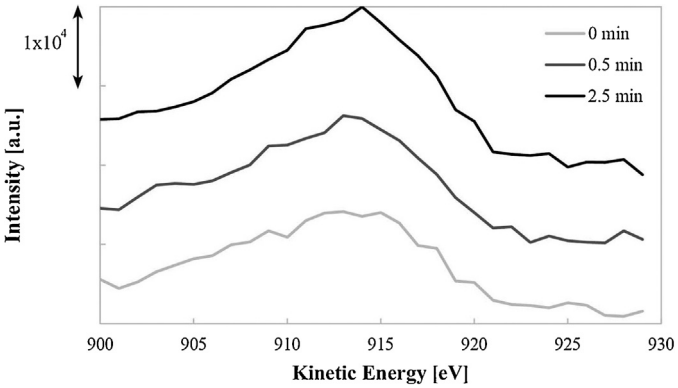

Fig. 7. Cu LVV spectra recorded at different depth of a Cu-rich zone of the Zr-based conversion film formed on the alkaline treated AA6014 specimen.

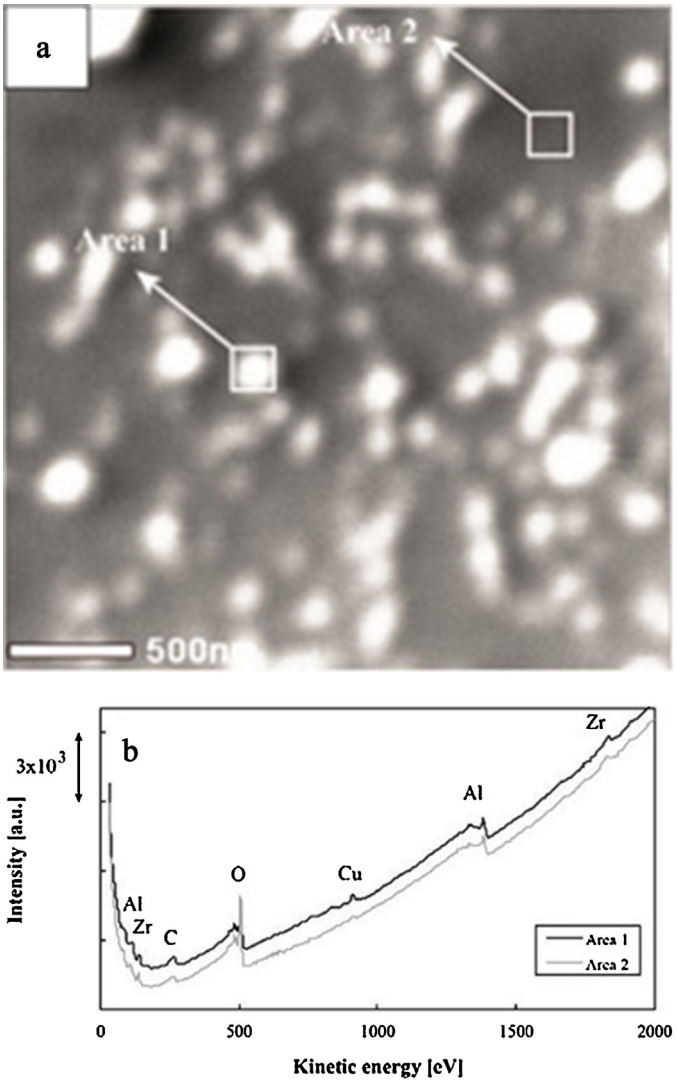

Fig. 8. (a) SEM micrograph of the Zr-based conversion film formed on the acid treated AA6014 specimen. (b) FE-AES spectra of two different areas of the sample.

establishing the color scale of the map as the intensity ((peak-background)/background) for each element. Additionally, depth profiles were obtained using argon sputtering at an energy level of 1 keV. The data were processed using the JEOL Image and Spectra Investigator software. Since the sputter rate related to the chemical composition and morphology of the matrix, the depth is presented as a function of the sputter time.

3. Results and discussion

3.1. FE-AES study of acidic and alkaline treated AA6014 samples

To study the local composition of the AA6014 specimen after the application of the surface conditioning treatments, FE-AES spectra were acquired on the different samples. Fig. 1(a) presents a SEM micrograph of the studied area of the reference sample. Several bright particles are present at the surface, with a size of less than 1 μm^2. Fig. 1(b) shows FE-AES spectra acquired on such a particle (area 1) and on a particle free zone of the surrounding Al matrix (area 2). The area 1-spectrum exhibits three peaks between 590 and 700 eV, which refer to Fe LMM transitions, and predominant signals around 1350 eV, which reflect Al KLL transitions. In the area-1 spectrum, the iron signals are missing and mainly Al is detected. It

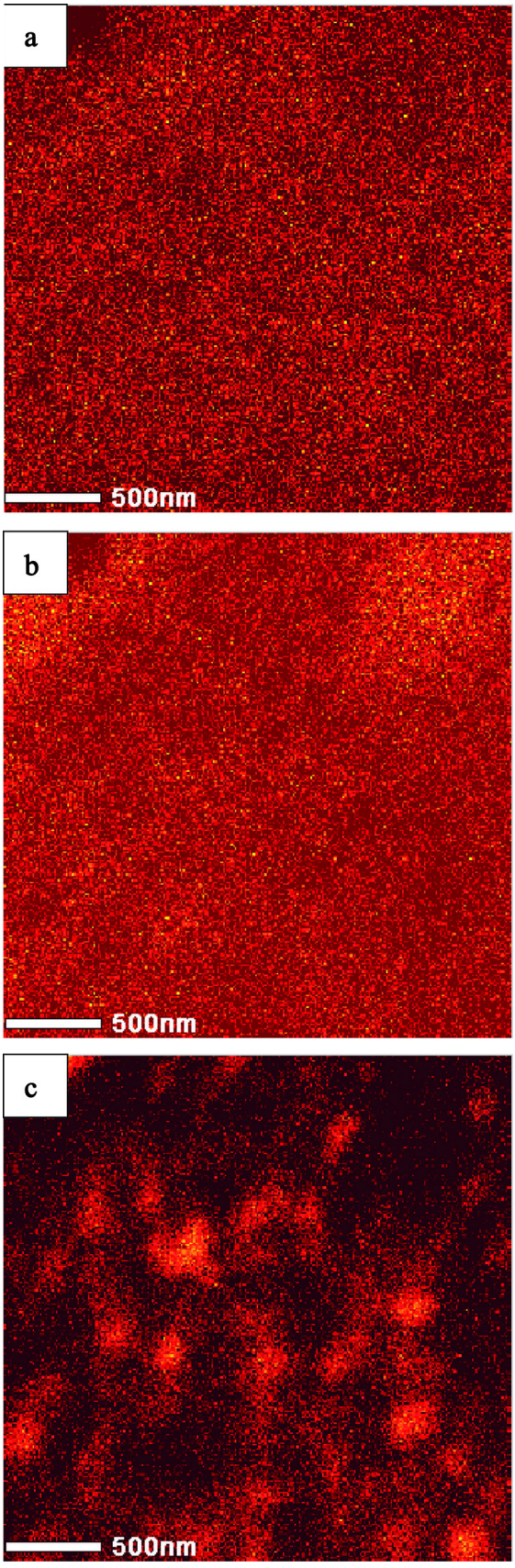

Fig. 9. FE-AES (a) Zr, (b) Al, (c) Cu map for the acid treated AA6014 aluminium alloy.

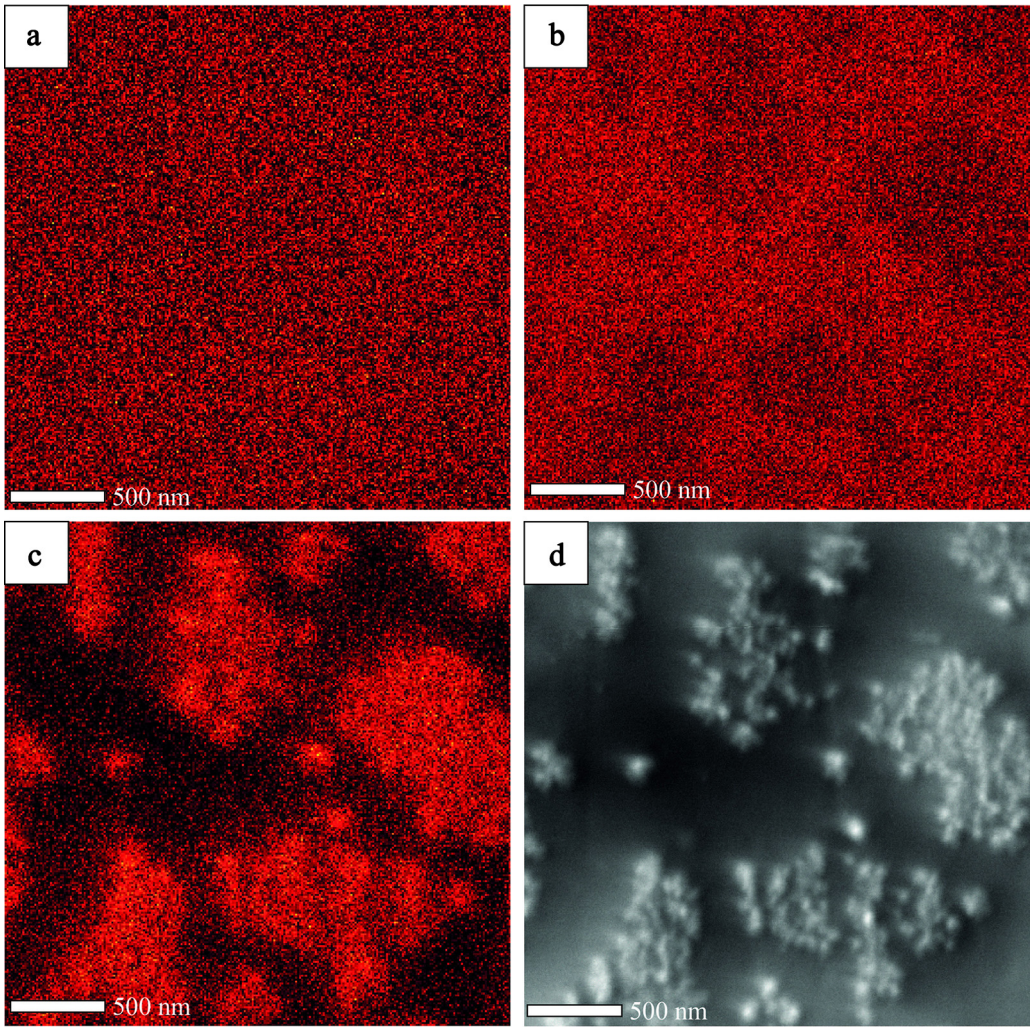

Fig. 10. FE-AES (a) Zr, (b) Al and (c) Cu map of the Zr-based conversion coatings deposited on the AA1050 alkaline treated sample. (d) SEM micrograph of the studied area.

should be noted that no traces of Cu were detectable on the surfaces of the Al reference samples.

Fig. 2(a) shows a SEM micrograph of the AA6014 alkaline treated specimen. The surface contains several round-shaped particles of 500 nm or less in diameter. FE-AES spectra were acquired inside and outside of these particles and the results are presented in Fig. 2(b). The areas in which the FE-AES spectra were acquired are indicated in Fig. 2(a). The FE-AES spectrum taken on the particle shows the presence of three peaks between 780 and 930 eV, which correspond to the Cu LMM transition. These signals clearly indicate a Cu-enrichment at the substrate surface and thereby confirm a release of copper species from the Al-alloy matrix and/or the embedded intermetallic particles during an immersion in alkaline solution.

The FE-AES analysis of the acidic treated AA6014 sample is presented in Fig. 3. Fig. 3(a) shows an SEM image of the overall investigated area. Marked zones refer to locations on which FE-AES spectra were acquired. In general, an intermetallic particle of 2 μm × 2 μm in size can be easily identified. On top of the intermetallic phase as well as in its vicinity, distinctly smaller and bright particle 'dots' seem to be distributed. Fig. 3(b) presents three FE-AES spectra recorded on the Al matrix (area 1), on a 'dot-free' zone of the intermetallic (area 2) and on one of the small bright particles (area 3). For area 1 majorly Al is detected (see the Al KLL peak), whereas the sample surface in area 2 mainly consists of iron (see the Fe LMM transitions). Interestingly, a significant amount of Cu is detected on the small particle dots in area 3 (see the Cu LMM signals). The presence of Cu-rich particles for the alkaline and acid treated specimens combined with the lack of Cu at the surface for the reference sample suggest a de-alloying process as a result of these surface conditioning treatments. It is important to note that conventional energy dispersive X-ray spectroscopy would indicate the presence of copper even for the reference sample due to its large penetration depth of several μm. FE-AES, in contrast, is extremely surface sensitive and just probes the first few nm of the sample-relevant Cu amounts hidden in the Al matrix beneath this surface layer will not contribute to the detected elemental composition.

FE-AES consequently shows that during immersion in acidic and alkaline solutions, initial dissolution of Cu-rich intermetallic particles occurs, followed by a re-deposition of Cu clusters around and further outside the site of origin due to the solution movement [21]. This Cu enrichment has been previously reported by Dimitrov et al. [22] for Al-Cu-Mg alloys that were in contact with alkaline solutions. Several authors have also shown the presence of Cu at the surface of different aluminium alloys after the exposure in acid solutions [23–26]. In this context, etching of the alloy surface in alkaline or acidic solution is an important prerequisite, because only the dissolution of a few nanometers of the Al matrix will excavate a relevant amount of intermetallics at the substrate surface, which can be subsequently subject to de-alloying [26]. Fig. 1 confirms this, because without etching, no Cu-rich intermetallics are detected.

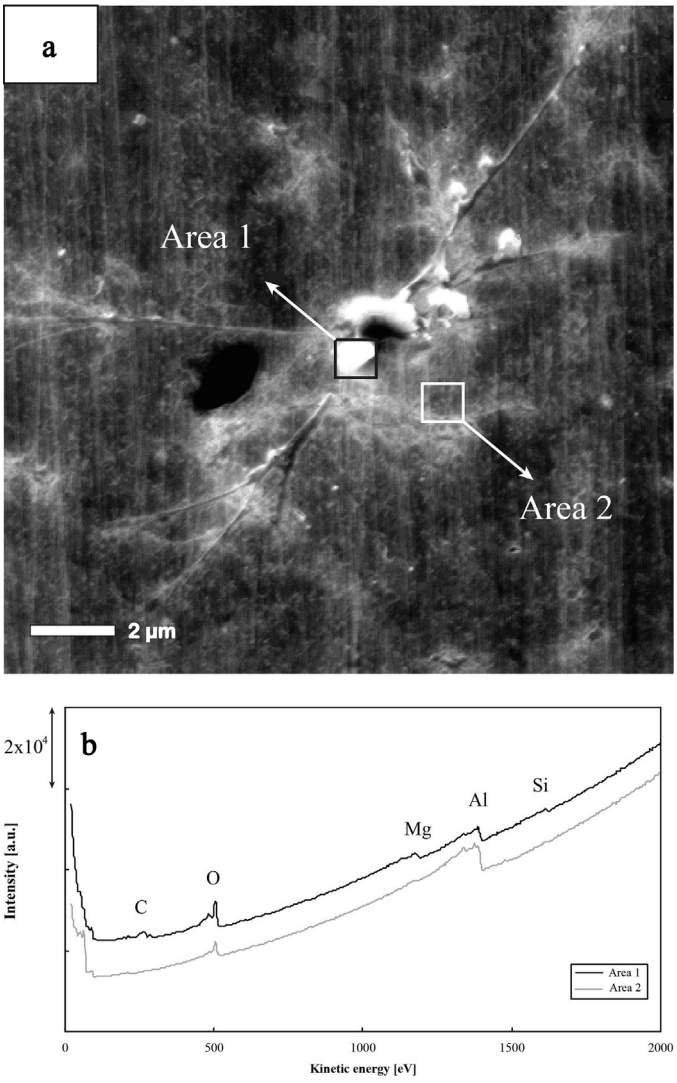

Fig. 11. (a) SEM micrograph of the AA6014 thermally treated specimen. (b) FE-AES spectra at two different locations of the sample.

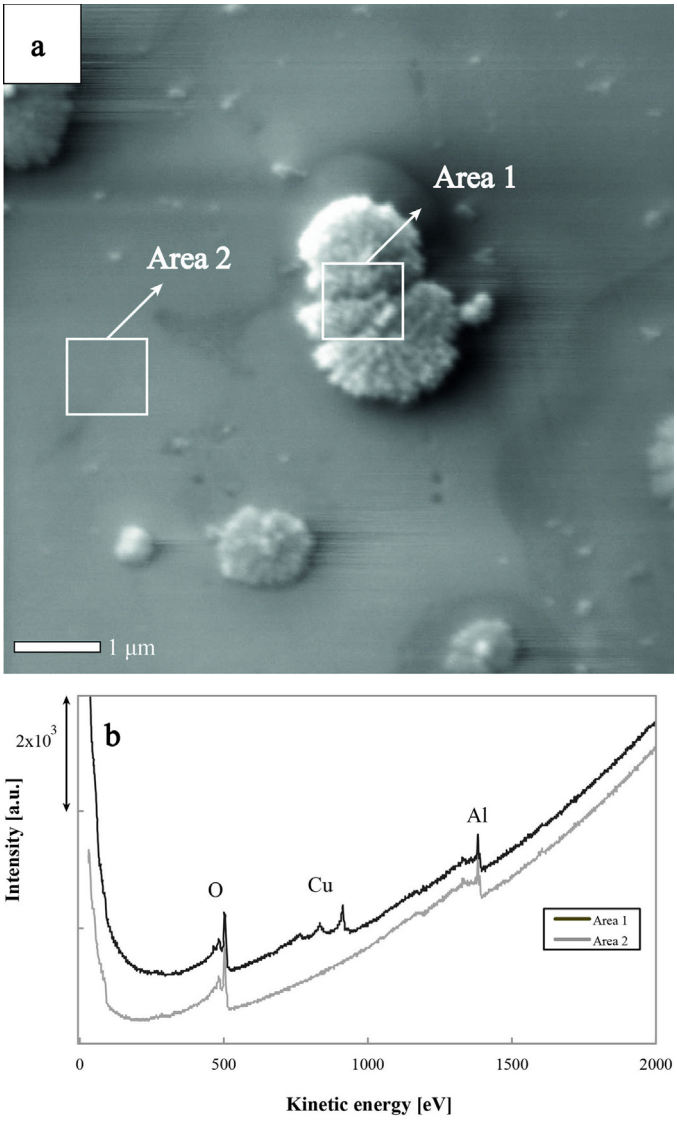

Fig. 12. (a) SEM micrograph of the Zr-based conversion coating formed on the AA6014 thermally treated specimen. (b) FE-AES spectra at two different areas of the sample.

3.2. FE-AES study of the Zr-based conversion coatings deposited on the acidic and alkaline treated aluminium alloys

To study the local elemental distribution of the Zr-based conversion coatings formed on the differently pre-conditioned aluminium alloys, FE-AES spectra, depth profiles and elemental maps were acquired. Fig. 4(a) shows a SEM micrograph of the AA6014 alkaline treated specimen after immersion in the conversion bath. Different bright round particles of 500 nm or less in diameter are observed. Fig. 4(b) presents FE-AES spectra that were acquired on these particles (area 1) and on the surrounding Al matrix (area 2). For both zones, Zr, Al, O and C are detected. The intensities of the different transitions for these elements are similar in both areas. Remarkably, Cu is only present on the bright areas. Fig. 5 shows FE-AES maps for Zr, Al and Cu that were recorded in the area of the SEM image of Fig. 4(a). These maps confirm a globally homogeneous distribution of Zr and Al, while Cu seems to be locally enriched in the form of agglomerates. It is clear that the Cu-rich zones correspond to the bright zones of Fig. 4(a). Based on the findings discussed in the previous section, the formation of Cu dots has to result from both de-alloying/re-deposition processes of Cu^{2+} during alkaline cleaning and additional precipitation of Cu-ions from the subsequently generated conversion coating layer. Comparing Fig. 2(a) with Fig. 4(a), the number of detectable Cu agglomerates does not seem to increase significantly by immersion in the conversion coating solution, however, their average size, does.

FE-AES depth profiles were recorded in zones with (Fig. 6a) and without the Cu enrichment (Fig. 6b) to study the film compositions in more detail. Zr, O, Al and C are predominant elements in both areas, but the layer structures nevertheless distinctly differ. A significant amount of Cu is only verifiable in Fig. 6(a). Its maximum is achieved at around 16 at% after about 2 min of sputtering, then slowly decays. The data point at a distribution of Cu throughout the entire conversion film with no specific enrichment at the interface between substrate and conversion layer. In Fig. 6(b), the amount of Zr decreases to half of its maximum value after 1 min of sputtering, whereas for Fig. 6(a), such decrease is not detected before 2 min of sputtering. This indicates that the thickness of the conversion film in Cu-rich zones is at least two times higher than the one obtained in regions without Cu deposits. Regarding the chemical state of the Cu agglomerates, FE-AE spectra do not indicate any change of oxidation states throughout the conversion layer. Fig. 7 presents Cu LVV peaks recorded in the Cu-rich zones of Fig. 6(a) before and after 0.5 and 2.5 min of argon sputtering, which refers

to signals recorded at the outer surface of the Zr-oxide layer and those obtained near the interface to the substrate. These peaks exhibit very similar shapes with an intensity maximum at 914 eV. They can be assigned to CuO [28,29] and confirm the results discussed by Sarfraz et al. [20]. Currently, it is not clear whether an initial oxidation of metallic Cu occurs in the course of conversion layer formation, an artifact resulting from sputtering during layer analysis or a combination of both phenomena [30].

Fig. 8(a) presents a SEM micrograph of the Zr-based conversion coating deposited on the AA6014 acidic treated specimen. Like in the case of the alkaline treated sample, it shows bright round-shaped particles of 500 nm or less in diameter. FE-AES spectra were acquired on these particles and the surrounding Al matrix. Fig. 8(b) shows that Zr, Al, C and O are verifiable in both regions, while Cu is only detected on the bright particle. Similar to the results shown in Fig. 4(b), the intensities of the Zr and Al peaks are similar for both of the studied regions.

Fig. 9 shows the corresponding FE-AES Zr, Al and Cu maps obtained for the surface section analyzed in Fig. 8. Similar to the alkaline treated specimen, all elements except the Cu are homogeneously distributed over the surface. Remarkably, the density of Cu-rich particles is distinctly higher. This finding clearly indicates that the amount of actively growing Cu-crystallization cores during conversion coating formation can be specifically tailored based on the type of pre-conditioning and cleaning.

Fig. 10 presents the FE-AES Zr, Al and Cu maps together of with SEM image of the studied area for Zr-based conversion layers formed on the AA1050 alkaline treated specimen. Like in the case of the acidic and alkaline treated AA6014, a homogeneous distribution of Zr and Al is obtained, while Cu precipitated inhomogeneously so that Cu-rich areas are observed for this sample, as well. Since the AA1050 is a Cu-free aluminium alloy, all Cu particles observed in Fig. 10(c) have to result from precipitation from the conversion coating solution.

3.3. *FE-AES surface morphology study of thermally pre-conditioned AA6014*

To further explore the importance of the Al-oxide layer structure on the interdependency of Cu precipitation and Zr-deposition kinetics during conversion coating, additional experiments were performed with thermally conditioned samples. Fig. 11(a) presents a SEM micrograph of a thermally treated AA6014 specimen. Different bright spots are observed on its surface. FE-AES spectra shown in Fig. 11(b) were acquired on these spots (area 1) as well as on the surrounding Al matrix (area 2). For area 2, mainly aluminium and oxygen signals were recorded, whereas additional peaks were recorded in the spectrum of area 1. With an energy of approximately 1150 eV and 1550 eV, they refer to Mg and Si KLL transitions and confirm an enrichment of magnesium and silicon at the surface due to their preferential oxidation at elevated temperatures during thermal treatment [27].

Fig. 12(a) presents a SEM micrograph of a thermally treated AA6014 sample after immersion in the conversion solution. Several round shaped particles of approximately 1 μm in diameter are present at the surface. Fig. 12(b) shows the FE-AES spectra acquired on one of the bright particles (area 1) and of the Al matrix (area 2). For area 1, Al KLL, Cu LMM and O KLL peaks appear in the spectrum, whereas no copper signals were obtained from area 2. As no de-alloying effects were observed on AA6014 after thermal pre-conditioning of the surface so that no Cu was precipitated, the conversion coating bath itself will be the only source for Cu deposition in the present case. Interestingly, no or almost no Zr is verifiable on the surface. This means that any preferential film formation effects for Zr-based conversion layers that may be mediated by Cu crystallization cores will be suppressed by the changes in the oxide film chemistry promoted by the exposure of the Al alloy to elevated temperatures. The reason of this behavior, as explained by Cerezo et al. [11], is linked to the interaction of free fluorides with the oxide film. This is an important observation, as Al-compounds can be subject to heat treatment procedures prior to thin-film deposition in the course of industrial manufacturing processes.

4. Conclusions

The effects of alkaline, acidic and thermal pre-conditioning treatments for AA6014 were investigated with respect to the layer characteristics of subsequently precipitated Zr-based thin film conversion coatings. Complementary data were obtained on copper-free AA 1050 surfaces. The following conclusions can be drawn:

Immersion of copper-containing AA6014 in acidic and alkaline solution results in de-alloying of embedded intermetallics particles, which results in dissolution and re-distribution of Cu-agglomerates on top of the intermetallics and across the surface of the surrounding Al matrix. As a result, active Cu crystallization cores are already present at the sample surface when it is immersed in Cu-containing hexafluorozirconic acid solution. During conversion coating, the Cu-rich particles do not seem to grow significantly in number, but in size. At and around the Cu-enriched zones, the resulting conversion coating thickness consequently occurs to be significantly increased, whereas the Zr amount was rather homogeneously distributed across the surface.

De-alloying only occurs if the pre-conditioning procedure induces etching of the AA6014 alloy surface. In that case, the conversion bath solution itself functions as the only source for Cu precipitation, but even under these conditions hardly any Zr deposition can be induced.

If Cu is absent in the AA alloy, in particular for AA1050, etching of the substrate surface, e.g. due to alkaline pre-conditioning, does not only allow for subsequent Cu deposition from the conversion bath solution, but also enables a correlated precipitation of zirconium species.

In general, it is shown that pre-conditioning/cleaning procedures on Al compounds allow specific control and adjustment of the distribution of Cu agglomerates on the surface. These Cu-rich zones have a strong impact on the local thickness of the conversion coating, but cannot stimulate the Zr deposition process if the surrounding Al oxide structure was not adequately activated before.

Acknowledgements

This research was carried out under the project number M22.6.10377 in the framework of the Research Program of the Materials innovation institute M2i (www.m2i.nl).

References

[1] G. Gusmano, G. Montesperelli, M. Rapone, G. Padeletti, A. Cusmà, S. Kaciulis, A. Mezzi, R. Di Maggio, Zirconia primers for corrosion resistant coatings, Surf. Coat. Technol. 201 (2007) 5822–5828.
[2] L. Fedrizzi, F.J. Rodriguez, S. Rossi, F. Deflorian, R. Di Maggio, The use of electrochemical techniques to study the corrosion behaviour of organic coatings on steel pretreated with sol–gel zirconia films, Electrochim. Acta 46 (2001) 3715–3724.
[3] L. Fedrizzi, F. Deflorian, P.L. Bonora, Corrosion behaviour of fluotitanate pretreated and painted aluminium sheets, Electrochim. Acta 42 (1997) 969–978.
[4] F. Mansfeld, Y. Wang, Development of "stainless" aluminum alloys by surface modification, Mat. Sci. Eng. A 198 (1995) 51–61.
[5] R. Posner, N. Fink, M. Wolpers, G. Grundmeier, Electrochemical electrolyte spreading studies of the protective properties of ultra-thin films on zinc galvanized steel, Surf. Coat. Technol. 228 (2013) 286–295.

[6] B. Tepe, B. Gunay, Evaluation of environmentally friendly Zr based nano structured conversion coating for HRS (hot rolled steel) in powder coating, Defect. Diffus. Forum. 283–286 (2009) 316–322.
[7] O. Lunder, F. Lapique, B. Johnsen, K. Nisancioglu, Effect of pre-treatment on the durability of epoxy-bonded AA6060 aluminium joints, Int. J. Adhes. Adhes. 24 (2004) 107–117.
[8] R. Posner, N. Fink, G. Giza, G. Grundmeier, Corrosive delamination and ion transport along stretch-formed thin conversion films on galvanized steel, Surf. Coat. Technol. 253 (2014) 227–233.
[9] P. Taheri, K. Lill, J.H.W. de Wit, J.M.C. Mol, H. Terryn, Effects of zinc surface acid-based properties on formation mechanisms and interfacial bonding properties of zirconium-based conversion layers, J. Phys. Chem. C 116 (2012) 8426–8436.
[10] P. Laha, T. Schram, H. Terryn, Use of spectroscopic ellipsometry to study Zr/Ti films on Al, Surf. Interface Anal. 34 (2002) 677–680.
[11] J. Cerezo, P. Taheri, I. Vandendael, R. Posner, K. Lill, J.H.W. de Wit, J.M.C. Mol, H. Terryn, Influence of surface hydroxyls on the formation of Zr-based conversion coatings on AA6014 aluminum alloy, Surf. Coat. Technol. 254 (2014) 277–283.
[12] L. Li, A.L. Desouza, G.M. Swain, In situ pH measurement during the formation of conversion coatings on an aluminum alloy (AA2024), Analyst 138 (2013) 4398–4402.
[13] S. Verdier, S. Delalande, N. van der Laak, J. Metson, F. Dalard, Monochromatized X-ray photoelectron spectroscopy of the AM60 magnesium alloy surface after treatments in fluoride-based Ti and Zr solutions, Surf. Interface Anal. 37 (2005) 509–516.
[14] F. Andreatta, A. Turco, I. De Graeve, H. Terryn, J.H.W. de Wit, L. Fedrizzi, SKPFM and SEM study of the deposition mechanism of Zr/Ti based pre-treatment on AA6016 aluminum alloy, Surf. Coat. Technol. 201 (2007) 7668–7685.
[15] O. Lunder, C. Simensen, Y. Yu, K. Nisancioglu, Formation and characterisation of Ti–Zr based conversion layers on AA6060 aluminium, Surf. Coat. Technol. 184 (2004) 278–290.
[16] J.H. Nordlien, J.C. Walmsley, H. Osterberg, K. Nisancioglu, Formation of a zirconium-titanium based conversion layer on AA 6060 aluminium, Surf. Coat. Technol. 153 (2002) 72–78.
[17] S. Adhikari, K.A. Unocic, Y. Zhai, G.S. Frankel, J. Zimmerman, W. Fristad, Hexafluorozirconic acid based surface pretreatments: characterization and performance assessment, Electrochim. Acta 56 (2011) 1912–1924.
[18] T. Lostak, S. Krebs, A. Maljusch, T. Gothe, M. Giza, M. Kimpel, J. Flock, S. Schulz, Formation and characterization of Fe^{3+}-/Cu^{2+}-modified zirconium oxide conversion layers on zinc alloy coated steel sheets, Electrochim. Acta 112 (2013) 14–23.
[19] J. Cerezo, I. Vandendael, R. Posner, K. Lill, J.H.W. de Wit, J.M.C. Mol, H. Terryn, Initiation and growth of modified Zr-based conversion coatings on multi-metal surfaces, Surf. Coat. Technol. 236 (2013) 284–289.
[20] A. Sarfraz, R. Posner, M.M. Lange, K. Lill, A. Erbe, Role of He intermetallics and copper in the deposition of ZrO_2 conversion coatings on AA6014, J. Electrochem. Soc. 161 (2014) C509–C516.
[21] R.G. Buchheit, Copper removal during formation of corrosion resistant alkaline oxide coatings on Al–Cu–Mg alloys, J. Appl. Electrochem. 28 (1998) 503–510.
[22] N. Dimitrov, J.A. Mann, M. Vukmirovic, K. Sieradzki, Dealloying of Al_2CuMg in alkaline media, J. Electrochem. Soc. 147 (2000) 3283–3285.
[23] R.G. Buchheit, R.P. Grant, P.F. Hlava, B. McKenzie, G.L. Zender, Local dissolution phenomena associated with S Phase (Al2CuMg) particles in aluminum alloy 2024-T3, J. Electrochem. Soc. 144 (1997) 2621–2628.
[24] R.G. Buchheit, M.A. Martinez, L.P. Montes, Evidence for Cu ion formation by dissolution and dealloying the Al_2CuMg intermetallic compound in rotating ring-disk collection experiments, J. Electrochem. Soc. 147 (2000) 119–124.
[25] S. Lebouil, J. Tardelli, E. Rocca, P. Volovitch, K. Ogle, Dealloying of Al_2Cu, Al_7Cu_2Fe, and Al_2CuMg intermetallic phases to form nanoparticulate copper films, Mater. Corros. 65 (2014) 416–424.
[26] W.B. Liu, S.C. Zhang, N. Li, J. Zheng, Y. Xing, Dealloying behavior of dual-phase Al 40 atom % Cu alloy in an alkaline solution, J. Electrochem. Soc. 158 (2011) D91–D94.
[27] S. Feliu Jr., M.J. Bartolomé, Influence of alloying elements and etching treatment on the passivating films formed on aluminium alloys, Surf. Interface Anal. 39 (2007) 175–180.
[28] D.A. Ramaker, The past, present, and future of auger line shape analysis, Crit. Rev. Solid State Mater. Sci. 17 (1991) 211–276.
[29] Y. Van Ingelgem, I. Vandendael, J. Vereecken, A. Hubin, Study of copper corrosion products formed during localized corrosion using field emission Auger electron spectroscopy Surf. Interface Anal. 40 (200) 273–276.
[30] W. Reuter, K. Wittmaack, An AES-SIMS study of silicon oxidation induced by ion or electron bombardment, Appl. Surf. Sci. 5 (1980) 221–242.